

PEOPLE'S DEMOCRATIC REPUBLIC OF ALGERIA  
MINISTRY OF HIGHER EDUCATION AND RESEARCH SCIENTIST  
MOHAMED BOUDIAF UNIVERSITY - M'SILA

FACULTY OF TECHNOLOGIE  
ELECTRICAL ENGINEERING DEPARTMENT  
N°:.....



FIELD: ST  
FILLIARY: **Electrical engineering**  
OPTION: **Renewable Energy**

**Master these's**

Thesis presented for obtaining Academic Master's degree

by:

**ZEROUAK Manal**

**BEHLOULI Imane**

Title

**Identification of Photovoltaic Module Parameters for  
Simulation Application**

Jury members:

Dr. Abdelmalek ZORIG

M'sila University

President

Dr. Amar GUICHI

M'sila University

Supervisor

Dr. Smail GHADBANE

M'sila University

Co-supervisor

Pr. Said BARKAT

M'sila University

Examiner

Academic year 2023/2024

**THANKS**

*First and foremost, we thank **Allah** for giving us the strength, courage, and patience throughout all these years of study, enabling us to complete this humble work.*

*We would like to express our heartfelt gratitude to **Mr. GUICHI Amar** and **Mr. GHADBANE Ismail** for supervising this thesis. We thank them for their time and the invaluable advice they generously provided. Their suggestions greatly facilitated this work. May **Allah** reward them greatly.*

*We extend our sincere thanks to all the teachers of the Electrical Engineering Department at the University of M'sila who have contributed, directly or indirectly, to our education. We would also like to thank the esteemed committee members for their interest in our work, for accepting to review our thesis, and for their valuable contributions in evaluating it.*

DEDICATION

*With great pride and gratitude, I first and foremost thank **Allah** for granting me success and guiding me through this journey.*

*I dedicate the fruit of my effort and graduation to the dearest people in my heart. To **my beloved mother**, who has been my support and anchor in every step, and to **my dear father**, who never spared his advice and guidance.*

*To my dear brothers **Adwi**, who has been like a second father to me, his wife and children Aya, Issam, and Ansam, and to my brothers **Hamoudi**, **Mehdi**, and **Abdo**, and my dear sisters **chayma** and **Marihane**, you are always my source of strength and inspiration.*

*I also dedicate this success to my dear friends **Imane**, **Ratiba**, **Hadil**, **Shamse**, and **Salma**.*

*To my dear colleagues in the renewable energy specialty .*

**ZEROUAK Manal**

DEDICATION

*I begin by thanking God Almighty and giving Him praise*

*I dedicate this modest work to:*

*To my dear mother, **Mariem Kerai**: Your unwavering tenderness and support have guided me in life and studies.*

*To my dear father, **Ali**: Your tireless efforts and sacrifices for my education are invaluable. This work is a testament to your enduring support*

*Likewise, I dedicate this work to:*

*To all members of the **Bahlouli family** and the **Kerai family**.*

*To my late uncle **Ibrahim**, may he rest in peace. I pray for mercy and forgiveness for him.*

*To all my friends who were always by my side and accompanied me throughout my academic journey: **salma, Ratiba, Romaissa, Chames, Hadil, Manal, Khoula, Chaima, Nessrine**.*

**BEHLOULI Imane**

<b>List of Figures</b>	<b>vi</b>
<b>List of Tables</b>	<b>viii</b>
<b>General introduction</b>	<b>1</b>
<b>1 Construction and Modeling of Photovoltaic Panels</b>	<b>3</b>
<b>Construction and Modeling of Photovoltaic Panels</b>	<b>3</b>
1.1 Photovoltaic energy history . . . . .	3
1.2 The photovoltaic effect . . . . .	4
1.3 Semiconductor . . . . .	4
1.3.1 Definition . . . . .	4
1.3.2 Formation of the PN junction . . . . .	5
1.4 Principal of photovoltaic conversion . . . . .	5
1.5 Different photovoltaic cell technologies . . . . .	6
1.6 Electrical characteristics of photovoltaic cell . . . . .	7
1.7 Association of photovoltaic cells . . . . .	8
1.7.1 Serial Association . . . . .	9
1.7.2 Parallel association . . . . .	9
1.7.3 Mixed Association (in series and parallel) . . . . .	10
1.8 Comparison between Different PV Models . . . . .	10
1.9 Modeling of a photovoltaic cell . . . . .	10
1.10 Influence of climatic conditions on a photovoltaic module . . . . .	14
1.10.1 Influence of solar radiation on a photovoltaic module . . . . .	14
1.10.2 Influence of temperature on a photovoltaic module . . . . .	14
1.11 Influence of Temperature on Series and Shunt Resistances . . . . .	14
1.12 Advantages and disadvantages of photovoltaic systems . . . . .	15
1.12.1 Advantages . . . . .	15
1.12.2 Disadvantages . . . . .	16
<b>2 PV Panel Parameter Extraction Techniques</b>	<b>17</b>

<b>PV panel Parameter Extraction techniques</b>	<b>17</b>
2.1 Solar cells I-V explicit equations . . . . .	17
2.1.1 Model parameters . . . . .	18
2.2 Identification of Photovoltaic Panel Parameters . . . . .	18
2.2.1 Analytical Methods . . . . .	19
2.2.2 Metaheuristic Methods . . . . .	20
2.3 Justification for Selecting Particle Swarm Optimization (PSO) for Photovoltaic Model Optimization . . . . .	24
2.4 Elements of Particle Swarm Optimization . . . . .	24
2.5 Mathematical PSO equations . . . . .	24
2.6 Explanation of Particle Swarm Optimization (PSO) Elements . . . . .	25
2.7 Conclusion . . . . .	26
<b>3 Simulating and Experimenting Results</b>	<b>27</b>
<b>Simulating and Experimenting results</b>	<b>27</b>
3.1 Panel Parameters Extraction Based on PSO Algorithm . . . . .	27
3.1.1 Fitness function . . . . .	28
3.1.2 Definition of parameters search space . . . . .	29
3.1.3 PSO parametrs definition . . . . .	29
3.1.4 PSO processing steps . . . . .	29
3.2 Simulation results . . . . .	29
3.3 Predicted I-V Characteristic Curve . . . . .	31
3.4 Impact of Temperature and Irradiance on PV Model Prediction . . . . .	32
3.5 Real panel parameters identification . . . . .	33
3.5.1 Sampling points data measurement . . . . .	33
3.5.2 I-V characteristic measurement setup . . . . .	33
3.5.3 sampling points data measurement procedure . . . . .	34
3.6 Conclusion . . . . .	36
<b>General Conclusion</b>	<b>37</b>
<b>Summary</b>	<b>39</b>
<b>Bibliography</b>	<b>40</b>
<b>Bibliographie</b>	<b>42</b>

## LIST OF FIGURES

1.1	the photovoltaic effect . . . . .	4
1.2	Generation of the electron-hole pair . . . . .	5
1.3	Schematic diagram of a PV cell . . . . .	5
1.4	Monocrystalline Solar Panels (Mono-Si) . . . . .	6
1.5	Polycrystalline Solar Panels . . . . .	7
1.6	Amorphous photovoltaic cell . . . . .	7
1.7	The current-voltage (I-V) characteristic . . . . .	8
1.8	Series association of photovoltaic cells . . . . .	9
1.9	Parallel association of photovoltaic cells . . . . .	9
1.10	Mixed association representing a typical arrangement for photovoltaic modules . . . . .	10
1.11	Ideal single diode model (1M3P) . . . . .	11
1.12	Second type of PV model (1M4P) . . . . .	12
1.13	Equivalent circuit of a real PV cell with a five-parameter model with a diode . . . . .	13
1.14	Influence of solar radiation on a photovoltaic module . . . . .	15
1.15	Influence of temperature on a photovoltaic module . . . . .	15
2.1	Single-diode model of a PV module . . . . .	17
2.2	Methods used in PV parameter extraction . . . . .	19
2.3	Categorizing metaheuristic algorithms used in PV parameter extraction . . . . .	20
2.4	The mechanism of the Genetic Algorithms (GA) . . . . .	21
2.5	The mechanism of the Whale Optimization Algorithm (WOA) . . . . .	21
2.6	Fuzzy logic architecture . . . . .	22
2.7	(a) Initialization of DE. (b) Mutation process of DE . . . . .	23
2.8	The mechanism of the Particle Swarm Optimization (PSO) . . . . .	23
2.9	Velocity formation and position update in PSO . . . . .	25
3.1	Flowchart of the PSO program . . . . .	30
3.2	The I-V characteristic curve of Panasonic PE240M-BBB panel under STC conditions . . . . .	31
3.3	The P-V characteristic curve of Panasonic PE240M-BBB panel under STC conditions . . . . .	31
3.4	Predicted I-V characteristic curve of the Panasonic Eco Solution PE240M-BBB panel . . . . .	32
3.5	Impact of temperature and irradiance on the photovoltaic current . . . . .	32

3.6	Predictive I-V Curve Showing the Impact of Temperature and Irradiance Using PSO-Extracted Parameters . . . . .	33
3.7	Laboratory Setup . . . . .	35
3.8	Real PV panel (ET-M53685) I-V curve . . . . .	35
3.9	Real and predicted I-V characteristic curve of ET-M53685 panel . . . . .	35

## LIST OF TABLES

1.1	Comparison of PV Module Models . . . . .	11
3.1	Search space area definitions . . . . .	29
3.2	Specification of the Panasonic Eco Solution PE240M-BBB at STC condition . . . . .	30
3.3	Obtained PV panel Parameters using PSO Algorithm . . . . .	31
3.4	Obtained PV panel Parameters for Panasonic PE240M-BBB Panel under 800 W/m <sup>2</sup> and 35°C . . . . .	33
3.5	Specifications of Module 85W at STC condition . . . . .	34
3.6	Obtained PV panel Parameters for setup panel ET-M53685 . . . . .	36

## GENERAL INTRODUCTION

The worldwide rise in electrical energy demand has led to a massive reliance on power generators to supply power to consumers. However, the negative environmental impact of burning fossil fuels for electricity production has triggered the need to reduce greenhouse gas emissions. As a result, there has been a shift towards cleaner forms of renewable energy, such as solar and wind technologies. Solar PV technology, in particular, is a popular renewable energy option with the capacity to provide cleaner, stable, scalable, and cost-effective electricity for years to come [1].

Solar energy has become increasingly attractive in recent times. The amount of solar energy that reaches the Earth's surface in a single day is ten times more than the total energy consumed by all the people on our planet in a year. Photovoltaic (PV) energy has significant potential to supply energy with minimal environmental impact, as it is clean and pollution-free [2].

Photovoltaic energy, derived from the direct conversion of solar radiation into electrical energy through photovoltaic cells, stands out as a promising alternative. This transformation, facilitated by the photovoltaic effect, generates an electromotive force when the cell surface is exposed to sunlight. The voltage generated varies depending on the material composition of the cell. When multiple photovoltaic cells are combined in series or parallel configurations, they form a photovoltaic generator with a non-linear current-voltage (I-V) characteristic. Additionally, the performance of PV systems is influenced by environmental factors such as irradiance and temperature [3].

The performance of PV systems is significantly influenced by outdoor environmental conditions. Therefore, accurately evaluating the PV array's performance during operation through measured current and voltage data is crucial for controlling and optimizing PV systems. Currently, three common PV models exist: the single diode model (SDM), double diode model (DDM), and three diode model (TDM). The accuracy of these models depends on key parameters, which are susceptible to aging and device failures in real-world applications. Hence, accurately identifying these parameters under varying conditions can enhance system efficiency [4]. Various methods, including analytical and metaheuristic approaches, have been employed to identify PV parameters, with metaheuristic algorithms proving particularly effective due to their global search capabilities and derivative-free nature [5].

This study introduces the application of the particles Swarm Optimization PSO method for parameter extraction from solar cells and photovoltaic modules. requiring no derivative calculations, making it

suitable for identifying parameters of unknown models such as photocurrent, saturation current, series resistance, parallel resistance, and ideality factor governing the current-voltage relationship of solar cells. The effectiveness of this approach is validated using real-world data to ensure accurate parameter estimation.

The manuscript is structured as follows: alongside a comprehensive introduction and conclusion summarizing the study, the work is divided into three chapters:

**The first chapter** explores into the historical evolution of photovoltaic energy, elucidating the underlying principles of the photovoltaic effect, semiconductor physics, and the various technologies employed in PV cell fabrication. Understanding these foundational concepts is essential for grasping the complexities of PV system modeling and parameter extraction techniques.

**In the second chapter** delves into the intricate process of extracting PV panel parameters, a crucial step in accurately simulating and optimizing PV systems. Through a meticulous examination of analytical and metaheuristic methods, including Particle Swarm Optimization (PSO), this chapter seeks to unravel the nuances of parameter identification and optimization, paving the way for enhanced PV system performance and efficiency.

**The final chapter** bridges theory into practice, as simulated and experimental. From the application of PSO algorithms to the prediction of I-V characteristic curves, to the evaluation of system performance under varying environmental conditions, this chapter offers valuable insights into the real-world application of PV system modeling and control techniques.

In summation, this thesis represents a comprehensive endeavor to advance our understanding of photovoltaic technology and its implications for sustainable energy generation. By delving into the intricacies of PV system construction, modeling, and control, this research aims to contribute to the ongoing discourse surrounding renewable energy innovation and pave the way for a more sustainable energy future.

## Introduction

The photovoltaic energy is the result of the direct transformation of sunlight into electric energy by means of cells, which are generally based on crystalline silicon, that is the most technologically and industrially advanced branch, indeed silicon is one of the most abundant elements on earth in the form of non-toxic silicon.

In this chapter, we will present photovoltaic energy by detailing its history, the photovoltaic effect, the principal of photovoltaic conversion, different photovoltaic cell technologies, their association and their modeling. Additionally, we will thoroughly discuss the influence of climatic parameters on a photovoltaic generator.

### 1.1 Photovoltaic energy history

Here are some important dates in the history leading to the emergence of photovoltaic power:

In 1839: French physicist Alexandre Edmond Becquerel discovered the photovoltaic effect, which allowed light-electricity conversion.

In 1873: Willoughby Smith discovered the photoconductivity of selenium.

In 1883: The American Charles Fritts exploited the discovery of the Becquerel to create the first photovoltaic cell.

In 1891: Baltimore inventor Clarence Kemp patented the first commercial solar water heater.

In 1905: Albert Einstein published his paper on the photoelectric effect (along with a paper on his theory of relativity). In 1916: Robert Millikan provided experimental proof of the photoelectric effect.

In 1932: Audobert and Stora discover the photovoltaic effect in cadmium sulfide (CdS).

In 1954: At Bell Labs, Daryl Chapin, Calvin Fuller, and Gerald Pearson create the silicon photovoltaic (PV) cell, the first solar cell that can convert enough solar energy into power to run common electrical appliances.

In 1957: Hoffman Electronics produced solar cells with an efficiency of 8%.

In 1983: Worldwide photovoltaic production exceeds 21.3 megawatts, with sales of more than \$250 million.

In 1986: ARCO Solar has announced the release of the G-4000, which marks a significant milestone as the world's first commercial thin-film power module.

In 1992: A significant development occurred with the successful operation of a 7.5-kilowatt prototype dish system, incorporating an advanced stretched-membrane concentrator.

In 2000: A remarkable event took place at the International Space Station (ISS), as astronauts commenced the installation of solar panels. This installation marked the deployment of the largest solar power array in space. Each "wing" of the array was comprised of 32,800 solar cells.

In 2013: The global production of photovoltaic (PV) modules surpassed 18 gigawatts peak (GWp).

In 2016: solar photovoltaic energy produced 375 TWh, which was a significant increase compared to the 246 TWh produced in 2015. This increase accounted for 1.6% of global production. The growth in solar photovoltaic energy was driven by price drops of up to 80% for solar PV modules, which led to a 47 GW increase in solar capacity worldwide.

In 2018: France opened Europe's first solar panel recycling plant.

In 2022: PV solar accounted for roughly 4.5% of total global electricity generation.

## 1.2 The photovoltaic effect

The photovoltaic effect is the direct production of electricity from light, it was first observed in 1839 by the French physicist Edmond Becquerel. However, it was not until the 1950s that researchers at Bell Labs in the United States could manufacture the first photopile, the primary element of a photovoltaic system [6].

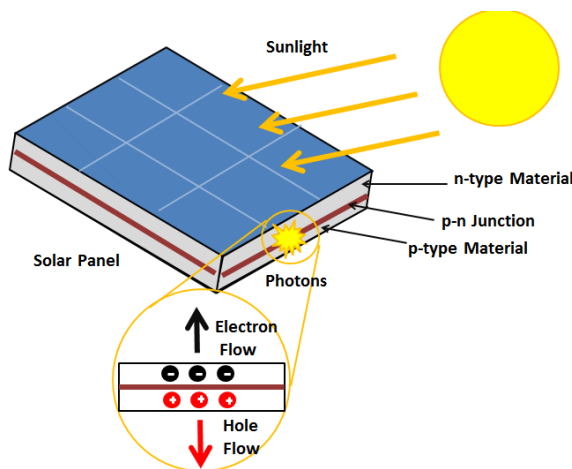


Figure 1.1: the photovoltaic effect

## 1.3 Semiconductor

### 1.3.1 Definition

Semiconductors are materials whose conductivity is intermediate between that of insulators and conductors. In semiconductors, conduction is ensured by two types of carriers electrons and holes [7]. The most advanced sector in terms of cells industry and technology is the production of silicon-based cells. Silicon is the most widely used semiconductor material because it is inexpensive and abundant on earth, making up 28% of the earth's crust in the form of silica, which is stable and non-toxic [8].

### 1.3.2 Formation of the PN junction

Silicon, like all semiconductors, has a full valence band and an empty conduction band. But with sufficient energy input, it is possible to move electrons from the valence band (VB) to the conduction band (CB), resulting in the generation of free electrons as shown in Figure (1.2).

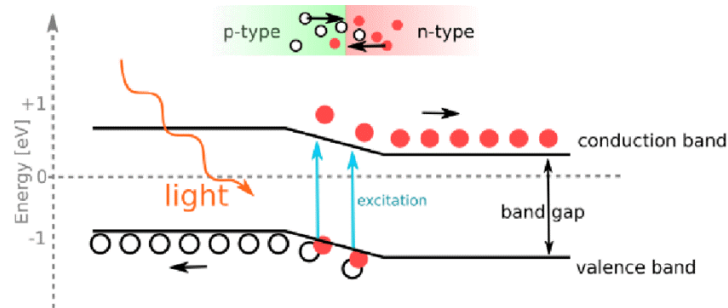


Figure 1.2: Generation of the electron-hole pair

The presence of free electrons in the conduction band of material is not enough to generate a current; it is necessary to create a potential difference at the terminals of the photo generator to drive the positive charges on one side and the negative charges on the other. This operation is possible by doping silicon. A PN junction is created by assembling two bars of N-type and P-type silicon. The component thus created is called a diode [8].

### 1.4 Principal of photovoltaic conversion

Photovoltaic conversion involves the direct transformation of solar irradiation into electrical current through the photovoltaic effect, utilizing solar cells. A typical PV cell comprises two semiconductor layers: one P-doped (boron-doped) and the other N-doped (phosphorus-doped), establishing a PN junction with a potential barrier. This junction facilitates the generation of an electric field within the cell. As electrons migrate to the positive P-side and holes to the negative N-side, an electric field is established, causing negatively charged particles to flow in one direction and positively charged particles in the opposite direction. Sunlight consists of photons, which are packets of electromagnetic radiation. When photons of suitable wavelengths interact with the cells, they transfer energy to electrons within the semiconducting material, promoting them to higher energy states within the conduction band. In this excited state, the electrons are mobile within the semiconductor material, generating an electric current within the PV cell [9].

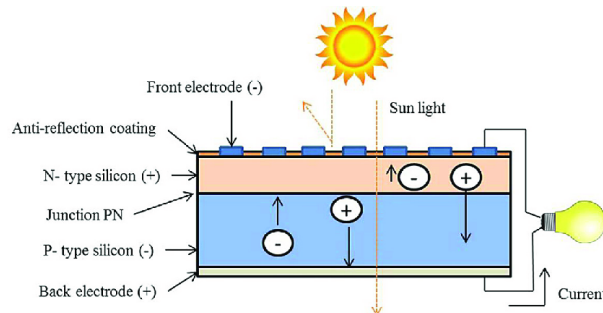


Figure 1.3: Schematic diagram of a PV cell

## 1.5 Different photovoltaic cell technologies

There are various technologies of solar cells available for converting sunlight into electrical energy. For power generation applications, the commercially available technologies are primarily based on silicon and can be categorized as either crystalline silicon or thin film. Each technology has different operating characteristics, conversion efficiencies, and costs [10].

### a) Monocrystalline Solar Cell (Mono-Si)

Monocrystalline photovoltaic solar panels have been the preferred choice for many years. They are renowned for being one of the oldest, most efficient, and reliable methods of generating electricity from sunlight. Monocrystalline solar cells are crafted from silicon ingots, which have a cylindrical shape. To enhance performance and reduce costs, manufacturers slice four sides off the cylindrical ingots to produce silicon wafers, giving monocrystalline solar panels their distinctive appearance. Figure (1.4) illustrates the monocrystalline solar panels [10].



Figure 1.4: Monocrystalline Solar Panels (Mono-Si)

### b) Multicrystalline silicon (Polycrystalline)

Polycrystalline silicon panels, as depicted in Figure (1.5), are characterized by the aggregation of crystals in various forms and directions. This unique structure gives rise to the iridescence observed in polycrystalline silicon cells, which is caused by the different orientations of the crystals and their consequent varying behavior with respect to light. The process of obtaining the polycrystalline silicon ingot involves melting and casting silicon into a parallelepiped-shaped mold. The resulting wafers are square-shaped and typically exhibit striations with a thickness ranging from 180 to 300  $\mu\text{m}$ .

While polycrystalline silicon panels have a lower efficiency compared to single-crystalline silicon (typically ranging from 12 to 14%), they also boast a lower cost, typically between 2.8 to 3.3 €/W. Despite the lower efficiency, polycrystalline silicon panels offer a long lifespan comparable to that of single-crystalline silicon panels, with maintenance of performance over time - retaining 85% of their initial efficiency even after 20 years [11].

### c) Amorphous cells



Figure 1.5: Polycrystalline Solar Panels

The amorphous silicon solar cell was the first thin-film solar cell. It has a simple form and a single p-i-n structure. This technology is commonly used in calculators and small electronic devices. The amorphous silicon solar cell is the most developed of the thin-film technologies [10].

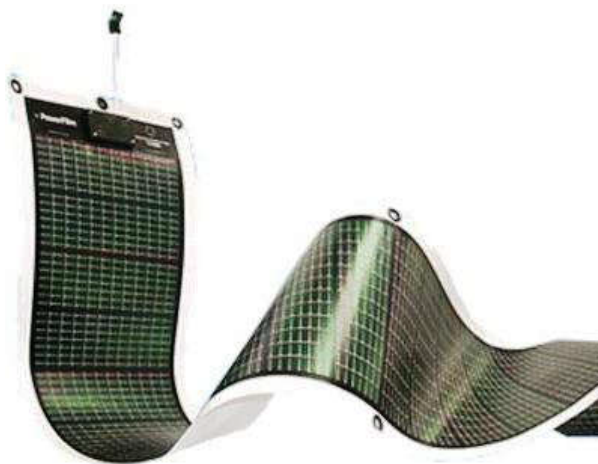


Figure 1.6: Amorphous photovoltaic cell

## 1.6 Electrical characteristics of photovoltaic cell

The electrical characteristics of a photovoltaic cell can be described by five parameters:

1. **Short-circuit current**  $I_{sc}$  (for  $V_{oc} = 0$ ):

The short-circuit current ( $I_{sc}$ ) is the current when the potential applied to the cell is zero ( $V = 0$ ). It is the maximum current that the cell can deliver. It depends on the illuminated area, the wavelength of the radiation, and the temperature.

## 2. Open circuit voltage $V_{oc}$ (for $I_{sc} = 0$ ):

The open-circuit voltage ( $V_{oc}$ ) is the voltage across the terminals of the cell when it is not connected to any load or connected to a load of infinite resistance ( $I = 0$ ).  $V_{oc}$  is given by the relationship:

$$V_{oc} = \frac{nkT}{q} \ln \left( \frac{I_{ph}}{I_0} + 1 \right) \quad (1.1)$$

## 3. Maximum Power Point (MPP):

The crucial section of the I-V characteristic for users is the one corresponding to energy generation. This point does not coincide with the open circuit voltage ( $V_{oc}$ ) or the short-circuit point, as they do not generate any power. Since power is the product of voltage and current ( $P = V \times I$ ), the maximum power point ( $V_{mp}$ ,  $I_{mp}$ ) represents the operating point at which the power supplied to the load reaches its maximum.

$$P_{mp} = V_{mp} \times I_{mp} \quad (1.2)$$

## 4. Fill factor (FF):

The fill factor (FF%) is used to characterize the quality of a PV cell or generator. This coefficient represents the ratio between the maximum power that the cell can deliver ( $P_{max}$ ) and the power formed by the rectangle  $I_{sc} \times V_{oc}$  Figure (1.7). It is defined by the following relation[3]:

$$FF = \frac{P_{mp}}{V_{oc} \times I_{sc}} = \frac{V_{mp} \times I_{mp}}{V_{oc} \times I_{sc}} \quad (1.3)$$

## 5. Efficiency ( $\eta$ ):

The efficiency  $\eta$  (%) of solar cells indicates the power conversion efficiency. It is the ratio between the maximum power delivered by the cell and the incident light power,  $P_{in}$ .

$$\eta = \frac{V_{mp} \times I_{mp}}{P_{in}} = \frac{FF \times V_{oc} \times I_{sc}}{P_{in}} \quad (1.4)$$

This efficiency can be improved by increasing the fill factor, the short-circuit current, and the open-circuit voltage. The conversion efficiency is a crucial parameter. Indeed, knowing its value alone allows for the evaluation of the cell's performance [10].

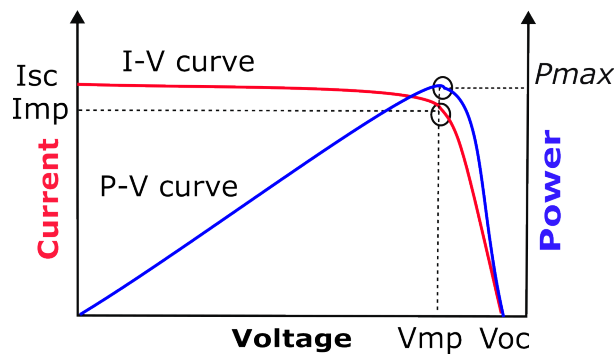


Figure 1.7: The current-voltage (I-V) characteristic

## 1.7 Association of photovoltaic cells

The power provided by a single solar cell being very low, several cells with similar characteristics must be electrically connected and encapsulated in plastic to form a practical PV array [12]. In the following, various possible configurations of solar cells are presented:

### 1.7.1 Serial Association

The series connection is depicted in Figure (1.8) and is characterized by the summation of individual cell voltages, while the output current is limited to that of the cell with the lowest photocurrent [12]. Equation (1.5) summarizes the electrical characteristics of a series connection of  $n_s$  cells [13]:

$$V_{oc\ ns} = n_s \times V_{oc} \quad \text{and} \quad I_{cc} = I_{cc\ ns} \quad (1.5)$$

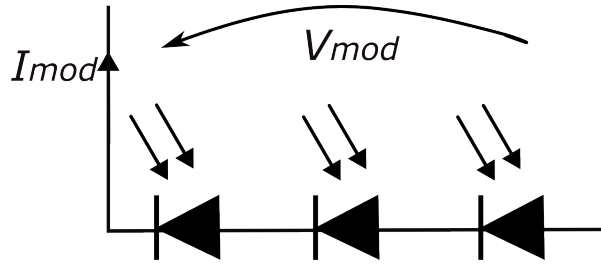


Figure 1.8: Series association of photovoltaic cells

The module voltage ( $V_{mod}$ ) and current ( $I_{mod}$ ) expressions are:

$$V_{mod} = \sum V_{cel} \quad (1.6)$$

$$I_{mod} = I_{cel} \quad (1.7)$$

Where:  $V_{cel}$  and  $I_{cel}$  are respectively the voltage and current of a PV cell.

### 1.7.2 Parallel association

The parallel association shown in Figure (1.9) is characterized by the addition of the currents of cells, or branches, connected in parallel, while the voltage at the output terminals is common to all cells, or branches [12].

Equation (1.8) summarizes the electrical characteristics of a parallel connection of  $n_s$  cells [13]:

$$I_{sc\ np} = n_p \cdot I_{sc} \quad \text{and} \quad V_{oc\ np} = V_{oc} \quad (1.8)$$

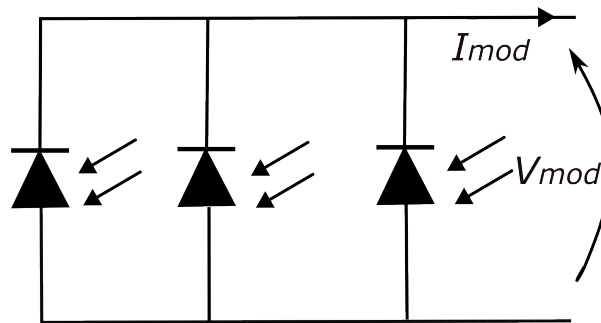


Figure 1.9: Parallel association of photovoltaic cells

The module voltage ( $V_{mod}$ ) and current ( $I_{mod}$ ) expressions are:

$$V_{mod} = V_{cel} \quad (1.9)$$

$$I_{mod} = \sum I_{cel} \quad (1.10)$$

### 1.7.3 Mixed Association (in series and parallel)

According to the series and/or parallel association of these cells, the values of the total short-circuit current and the total open-circuit voltage are given by the following relationships [10]:

$$I_{sc}^t = n_p \cdot I_{sc} \quad (1.11)$$

$$V_{oc}^t = n_s \cdot V_{oc} \quad (1.12)$$

Figure (1.10) shows the resulting characteristic obtained by associating identical cells in series ( $n_s$ ) and in parallel ( $n_p$ ).

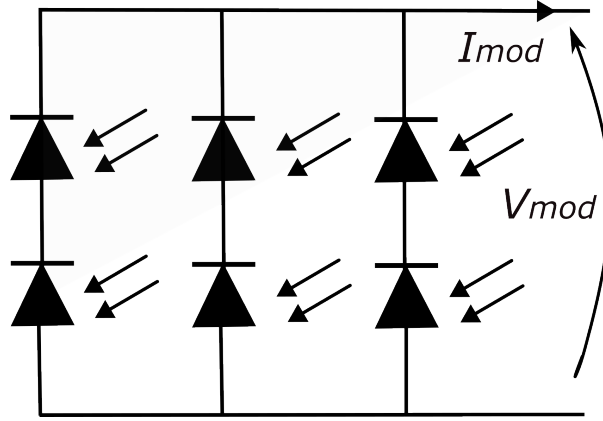


Figure 1.10: Mixed association representing a typical arrangement for photovoltaic modules

The module voltage ( $V_{mod}$ ) and current ( $I_{mod}$ ) expressions are:

$$V_{mod} = \sum V_{cel} \quad (1.13)$$

$$I_{mod} = \sum I_{cel} \quad (1.14)$$

## 1.8 Comparison between Different PV Models

Table (1.1) compares the three main types of PV modules, highlighting the primary advantages and disadvantages of each model. This comparison is crucial for understanding the differences between PV models. The three types of models are SDM, DDM, and TDM, with their main distinction being the accuracy of PV module performance representation. TDM has the highest accuracy as it accounts for most phenomena within the PV module, followed by DDM with intermediate accuracy, and SDM with the least accuracy [5]. In our work, we use the SDM model. Despite its lower accuracy compared to TDM and DDM, SDM is chosen due to its simplicity, reduced computational requirements, and ease of implementation. These factors make SDM a practical choice for our specific application, where these advantages outweigh the need for higher accuracy.

## 1.9 Modeling of a photovoltaic cell

The one of many models for representation the PV cell, the general adopted model is single-diode model [14]. three models of the PV cell will be presented:

1. Ideal diode model(1M3P);

Table 1.1: Comparison of PV Module Models

Model	Advantages	Disadvantages	Field of Application
SDM	<ul style="list-style-type: none"> <li>• Simple structure,</li> <li>• Low complexity,</li> <li>• Less calculation burden,</li> <li>• Easy to implement in the laboratory.</li> </ul>	<ul style="list-style-type: none"> <li>• Poor accuracy,</li> <li>• Unable to predict PV module performance under partial shading,</li> <li>• Less accurate in predicting the I-V curve.</li> </ul>	<ul style="list-style-type: none"> <li>• The most widely used model due to its simplicity,</li> <li>• Suitable in case fast estimation is needed with low manufacturing cost.</li> </ul>
DDM	<ul style="list-style-type: none"> <li>• Higher in accuracy compared to SDM,</li> <li>• Acceptable performance,</li> <li>• Easy to implement in the laboratory.</li> </ul>	<ul style="list-style-type: none"> <li>• More complex in structure,</li> <li>• High implementation cost in the laboratory.</li> </ul>	<ul style="list-style-type: none"> <li>• Suitable in case accurate I-V estimation is needed,</li> <li>• Can easily consider the variations of environmental conditions during simulation.</li> </ul>
TDM	<ul style="list-style-type: none"> <li>• Highest accuracy compared to the previous two models,</li> <li>• Models most of the phenomena in the PV module during performance.</li> </ul>	<ul style="list-style-type: none"> <li>• More complex than the other two models,</li> <li>• Large calculation time burden,</li> <li>• Complex concerning hardware implementation.</li> </ul>	<ul style="list-style-type: none"> <li>• For predicting values with high accuracy,</li> <li>• Can easily model the complex nature of different PV module types.</li> </ul>

2. Four-parameters model (1M4P);

3. Five-parameters model (1M5P).

### 1. Ideal diode model (1M3P):

PV cell has an exponential behavior disposal akin to a diode. The optimal model is shown in Figure (1.11) and consisting from (parallel connection of current source parallel with single diode). Called (1M3P) and has three parameters ( $I_0$ ,  $n$ ,  $I_{pv}$ ) [14].

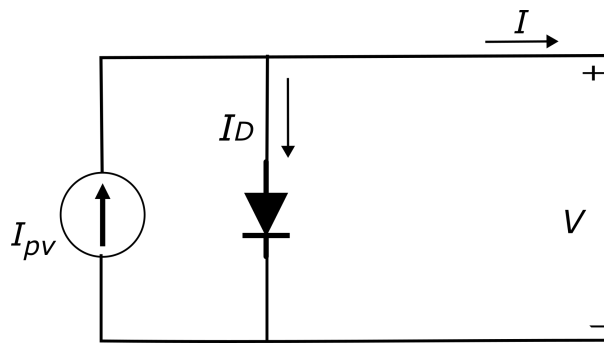


Figure 1.11: Ideal single diode model (1M3P)

Applying Kirchhoff law:

$$I = I_{pv} - I_D \quad (1.15)$$

The current of an ideal diode in darkness is given by the following relation:

$$I_D = I_0 \left( e^{\frac{qv}{nkT}} - 1 \right) \quad (1.16)$$

By combining the two previous equations, we obtain the general equation of this model:

$$I = I_{pv} - I_0(e^{\frac{qv}{nkT}} - 1) \quad (1.17)$$

Is<sub>c</sub> and Voc are depicted as:

$$I_{sc} = I_{pv} = I \text{ for } V = 0 \quad (1.18)$$

$$V = V_{oc} = \frac{nkT}{q} \ln\left(1 + \frac{I_{sc}}{I_0}\right) \text{ for } I = 0 \quad (1.19)$$

The output power is :

$$P = V[I_{sc} - I_0(e^{\frac{qv}{nkT}} - 1)] \quad (1.20)$$

With:

- $I(I_L)$ : Photocurrent.
- $I_D$ : Recombination current in the depletion region (junction region).
- $I_0$ : Diode saturation current.
- $n$ : Ideality factor of the diode.
- $k$ : Boltzmann constant ( $1.38 \times 10^{-23}$  J/K).
- $q$ : Electric charge (of an electron) (in coulombs).
- $T$ : Temperature in Kelvin.

## 2. Four-parameters model (1M4P):

The second type of PV model has four parameters ( $R_s$ ,  $I_0$ ,  $n$ ,  $I_{pv}$ ) as shown in Figure (1.12) [14].

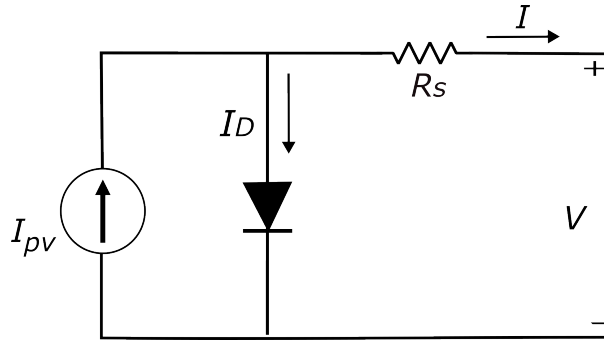


Figure 1.12: Second type of PV model (1M4P)

The characteristic equation is directly derived from Kirchoff's laws:

$$I = I_{pv} - I_D \quad (1.21)$$

The diode current is given by the following formula:

$$I_D = I_0(e^{\frac{qv + R_s I}{nkT}} - 1) \quad (1.22)$$

The general equation obtained by substituting equation (1.22) into equation (1.21) is:

$$I = I_{pv} - I_0(e^{\frac{qv + R_s I}{nkT}} - 1) \quad (1.23)$$

This model concludes the equation recurrent in order to find the voltage value at positive value of current.

### 3. Five-parameters model (1M5P):

The model consists of a constant current source, in parallel with a diode, which incorporates an ideality factor to account for recombination in the space-charge region. This model not only considers losses due to the module's internal series resistance but also accounts for losses associated with contacts and interconnections between cells and modules. Additionally, the shunt resistance of the module represents losses due to leakage currents across the junction and within the cell caused by crystal imperfections and impurities. This model strikes a good balance between approximation precision and simplicity [15].

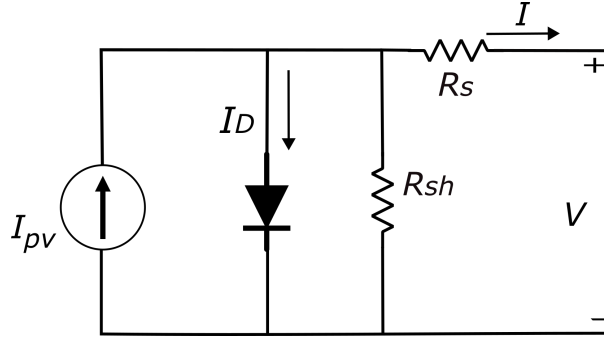


Figure 1.13: Equivalent circuit of a real PV cell with a five-parameter model with a diode

Using the equivalent circuit shown in Figure (1.13) and applying Kirchhoff's laws, we will have the following equations:

$$I = I_{pv} - I_D - I_{sh} \quad (1.24)$$

The diode current is given by the following formula:

$$I_D = I_0 \left( e^{\frac{qv + R_s I}{nkT}} - 1 \right) \quad (1.25)$$

The current of the parallel resistance is given by the relation:

$$I_{sh} = \frac{V + R_s I}{R_{sh}} \quad (1.26)$$

We substitute equations (1.25) and (1.26) into equation (1.24) and obtain the general equation of this model:

$$I = I_{pv} - I_0 \left( e^{\frac{qv + R_s I}{nkT}} - 1 \right) - \frac{V + R_s I}{R_{sh}} \quad (1.27)$$

when considering specific operating temperature  $T$ , the behavior of a photovoltaic panel is influenced in various ways. For instance, the short-circuit current  $I_{sc,e}(T)$  and open-circuit voltage  $V_{oc,e}(T)$  can be estimated using the following equations:

$$I_{sc,e}(T) = I_{scn} + KI_{sc}\Delta T \quad (1.28)$$

$$V_{oc,e}(T) = V_{ocn} + KV_{oc}\Delta T \quad (1.29)$$

And:

$$\Delta T = T - T_n \quad (1.30)$$

Where  $I_{scn}$  and  $V_{ocn}$  represent the short-circuit current and open-circuit voltage under nominal conditions, respectively. The coefficients  $KI_{sc}$  and  $KV_{oc}$  denote the short-circuit voltage and open-circuit voltage temperature coefficients. These coefficients are typically provided in the manufacturer's datasheet.

The intensity of light  $G$  and the operating temperature  $T$  both influence the photovoltaic current  $I_{pv}$ , which can be expressed as:

$$I_{pv} = \frac{G}{G_n}(I_{pvn} + KI_{sc}\Delta T) \quad (1.31)$$

Where,  $I_{pvn}$  represents the photovoltaic current under nominal conditions,  $KI_{sc}$  is the short-circuit current temperature coefficient, and  $\Delta T$  is the deviation of the operating temperature from the nominal temperature [16].

## 1.10 Influence of climatic conditions on a photovoltaic module

There are several factors that affect the solar panel efficiency, the most prominent of which are the solar radiation intensity and the PV panel temperature, which are closely related to each other and directly affect the efficiency and the output power of the solar panel. Usually, photovoltaic panels are manufactured under standard test conditions (STC), where it indicates that one-degree increase of temperature causes a decrease in the PV panel efficiency by 0.004-0.005. In the actual operating conditions of PV modules, these panels are not likely to operate under standard conditions. Therefore, when initiating the construction and installation of PV systems, real external conditions and exposure to different environmental conditions must be taken into account [17].

### 1.10.1 Influence of solar radiation on a photovoltaic module

As a function of the irradiance incident on the PV cells, the characteristic curve  $V - I$  of them changes as shown in Figure (1.14). When the irradiance decreases, the generated PV current decreases proportionally, whereas the variation of the no-load voltage is very small. As a matter of fact, the conversion efficiency is not influenced by the variation of the irradiance within the standard operation range of the cells, which means that the conversion efficiency is the same both in a clear as well as in a cloudy day. Therefore, the smaller power generated with a cloudy sky is referable not to a drop in the efficiency but to a reduced generation of current because of lower solar irradiance [11].

### 1.10.2 Influence of temperature on a photovoltaic module

Contrary to the previous case, when the temperature of the modules increases, the produced current remains practically unchanged, whereas the voltage decreases and with it, there is a reduction in the performance of the panels in terms of produced electric power (see Figure 1.15) [11].

## 1.11 Influence of Temperature on Series and Shunt Resistances

The series resistance ( $R_s$ ) of a solar cell decreases as the temperature increases. This occurs because higher temperatures lead to increased conductivity of the metal components within the solar cell module. Conversely, the shunt resistance ( $R_{sh}$ ) of a solar cell tends to increase with rising temperature. This increase is due to the decrease in recombination speed at the junction under open-circuit conditions as

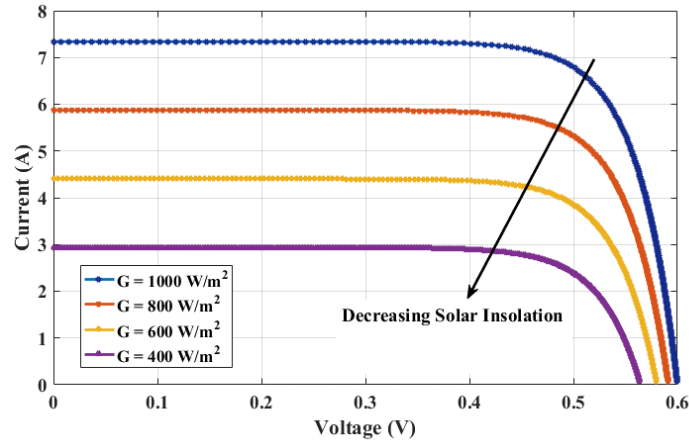


Figure 1.14: Influence of solar radiation on a photovoltaic module

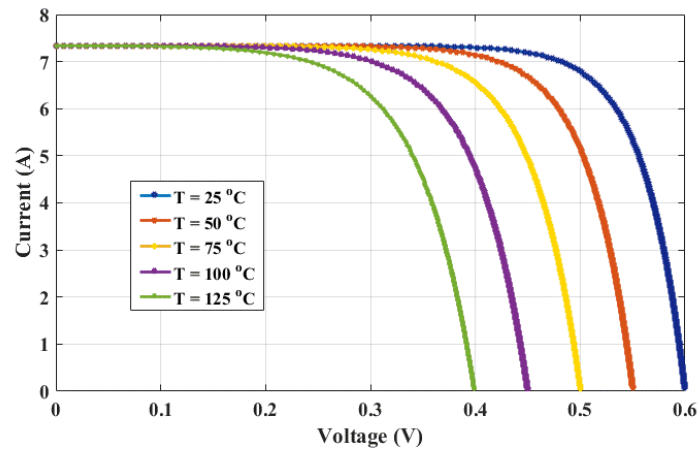


Figure 1.15: Influence of temperature on a photovoltaic module

the temperature rises. Shunt resistance is a crucial parameter that indicates the quality of the solar cell material and influences the cell's efficiency[18].

## 1.12 Advantages and disadvantages of photovoltaic systems

Photovoltaic systems offer numerous advantages, but they also have certain drawbacks, which are discussed in the following subsections.

### 1.12.1 Advantages

- The modular nature of photovoltaic panels allows for simple installation adaptable to various energy needs. Systems can be sized for power applications ranging from milliwatts to megawatts.
- Operating costs are very low due to minimal maintenance requirements, and it requires no fuel, transportation, or highly specialized personnel.
- Lastly, photovoltaic technology exhibits ecological qualities as the end product is non-polluting, silent, and does not cause any disruption to the environment, except for the use of space for large-scale installations [19].

### 1.12.2 Disadvantages

- The manufacturing of photovoltaic modules involves high technology and requires costly investments.
- The actual conversion efficiency of a module is low, typically around 10-15%, with a theoretical limit for a cell of 28%. Photovoltaic generators are not competitive compared to diesel generators except for low energy demands in isolated regions.
- When electrical energy storage in chemical form (battery) is necessary, the cost of the generator increases.
- Electrical energy storage still poses numerous challenges. The low efficiency of photovoltaic panels is explained by the operation of the cells themselves. To move an electron, the energy of the radiation must be at least 1 eV. Thus, all incident rays with lower energy will not be converted into electricity. Similarly, light rays with energy higher than 1 eV will lose this energy, with the remainder being dissipated as heat [19].

## Conclusion

This chapter addressed various aspects of solar energy, beginning with a presentation of its historical development. Subsequently, the photovoltaic effect was clarified. The second part of this chapter was dedicated to explaining the PN junction, as it is the main semiconductor junction that reflects the behavior of PV cells. Next, the principle behind solar energy was detailed, along with an exploration of the different types of solar cells and their various associations. The third part of this chapter focused on the mathematical modeling of PV cells, with the four known models clearly detailed. Finally, the chapter concluded by discussing the climatic effects on PV cells.

## Introduction

This chapter explores various optimization techniques aimed to extract photovoltaic panel parameters that are crucial for PV panel modeling. The identification methods used in the literature will be classified into two types: analytical and metaheuristic methods.

In this chapter, the most commonly used methods among the two types will be cited, and the metaheuristic ones will receive further clarification. Specifically, Particle Swarm Optimization (PSO), considered a metaheuristic method with numerous advantages compared to others, will be detailed more in-depth as it is chosen to be applied in this work.

### 2.1 Solar cells I-V explicit equations

As detailed in the first chapter, the equivalent circuit of the five parameters PV model ( $R_{sh}$ ,  $I_{sh}$ ,  $R_s$ ,  $m$ ,  $I_{ph}$ ) is depicted in Figure (2.1) [14], The effects of each parameter on the model will be clarified in the following section.

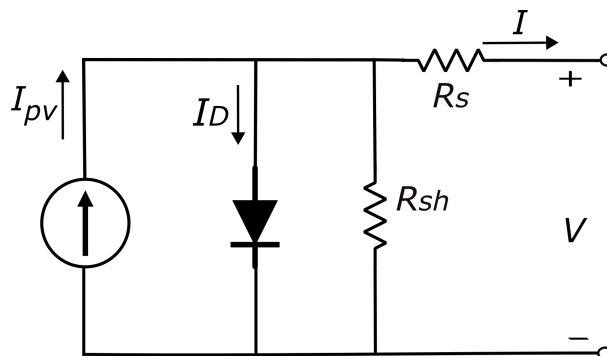


Figure 2.1: Single-diode model of a PV module

### 2.1.1 Model parameters

The physical and electrical significance and impact of PV cell (module) parameters can be outlined as follows:

**1. Ideality Factor ( $n$ ):**

The ideality factor ( $n$ ) is a unitless parameter. It measures how closely the diode follows the ideal diode equation, taking into account the various mechanisms responsible for moving carriers across the junction. A value of  $n$  equal to “one” indicates that the transport process is predominantly due to diffusion, while a value of “two” suggests that it is primarily due to recombination in the depletion region [20].

**2. Photo Current ( $I_{ph}$ ):**

As its appellation suggests, photocurrent is the current generated due to the absorption of photons by a solar cell [20]. When photons of light strike the solar cell, they transfer their energy to electrons in the material, causing them to move and create an electric current. This flow of electrons constitutes photocurrent and is fundamental to how solar cells convert light into electricity.

**3. Diode saturation current ( $I_0$ ):**

The diode saturation current, also known as the reverse saturation current, is the result of two primary mechanisms: thermal generation and minority carrier diffusion. Thermal generation occurs within the depletion region of the diode, where electron-hole pairs are spontaneously created due to thermal energy. Additionally, minority carriers in the  $n$  and  $p$  regions diffuse across the depletion region, contributing to the saturation current [20].

**4. Series resistance ( $R_s$ ):**

Series resistance in a solar cell stems from three primary sources: first, current flow through the emitter and base; second, contact resistance between the metal contact and silicon; and finally, resistance from the top and rear metal contacts. The primary consequence of series resistance is a reduction in the fill factor, though exceptionally high values may also diminish the short-circuit current [20].

**5. Parallel resistance ( $R_{sh}$ ):**

Significant power losses attributed to the presence of a shunt resistance are typically a result of manufacturing defects rather than poor solar cell design. Low shunt resistance leads to power losses in solar cells by offering an alternative current path for light-generated current. This diversion diminishes the current flowing through the solar cell junction, consequently reducing the solar cell's voltage. The impact of a shunt resistance is particularly pronounced at low light levels, as there is less light-generated current available. Consequently, the loss of this current to the shunt has a more substantial effect. Furthermore, at lower voltages where the solar cell's effective resistance is high, the influence of a resistance in parallel becomes significant [20].

## 2.2 Identification of Photovoltaic Panel Parameters

It is well known that the parameter determination phase of any system is a critical step for both simulation and practical purposes. Therefore, akin to any system, precise knowledge of PV panel parameters is essential for design, quality control, and performance estimation. These parameters are often deduced from experimental data under well-controlled lighting and temperature conditions. Manufacturers of PV

cells and panels typically furnish a datasheet containing some parameters of a PV cell or panel composed of an array of several cells. However, certain parameters are not provided in the datasheet. In practice, determining these unknown parameters is of utmost importance. In the literature, various techniques have been employed to extract PV cell model parameters, accommodating models with five, seven, or nine parameters. These techniques can be categorized into two primary types: analytical and metaheuristic methods, each encompassing several techniques as depicted in Figure (2.2). These techniques utilize the following PV cell (panel) parameters ( $I_{PV}$ ,  $I_0$ ,  $R_s$ ,  $R_{sh}$ ,  $n$ ) as inputs, to deliver, after processing, the following estimated parameters ( $I_{PV}$ ,  $I_0$ ,  $R_s$ ,  $R_{sh}$ ,  $n$ ), contingent upon the number of parameters adopted in the model [21].

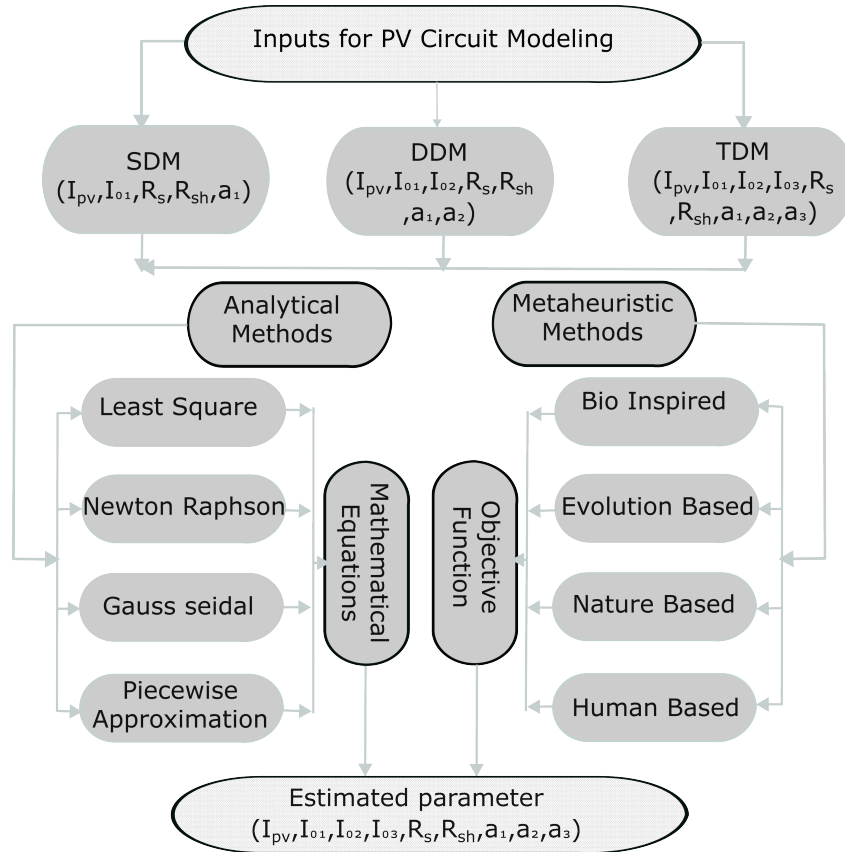


Figure 2.2: Methods used in PV parameter extraction

The definition of the two primary types, analytical and metaheuristic methods, will be elaborated upon in the following subsections.

### 2.2.1 Analytical Methods

Analytical methods for solar photovoltaic (PV) parameter extraction involve simplified calculations that require minimal computational effort. These methods are straightforward to construct and rely on simplifications or approximations, which can significantly affect the results. By combining various operating conditions with manufacturer datasheet values, analytical methods can determine the nonlinear characteristics of solar PV systems [22].

These methods aim to extract parameters explicitly by approximating certain terms in the system equations. They are known for their reliability, accuracy, and simplicity. However, they come with drawbacks. Primarily, they provide approximate solutions rather than exact ones. Additionally, they

often require specific information, such as the slopes of the I-V curve at the short circuit point, the open circuit point, and the maximum power point. Accurately measuring these values in practice can be challenging [23].

## 2.2.2 Metaheuristic Methods

Metaheuristic optimization algorithms are mathematical tools used to solve complex optimization problems. These algorithms aim to find or develop a sufficiently good solution to an optimization problem, particularly when information is sparse, inaccurate. Utilizing metaheuristics to enhance the performance of modern power systems is an appealing topic [23]. In Figure (2.3), the details of the metaheuristic algorithms are presented, categorized based on their sources of inspiration. These categories reflect the diverse inspirations behind each algorithm. Unlike analytical methods, metaheuristic algorithms require an objective function as a stopping criterion.

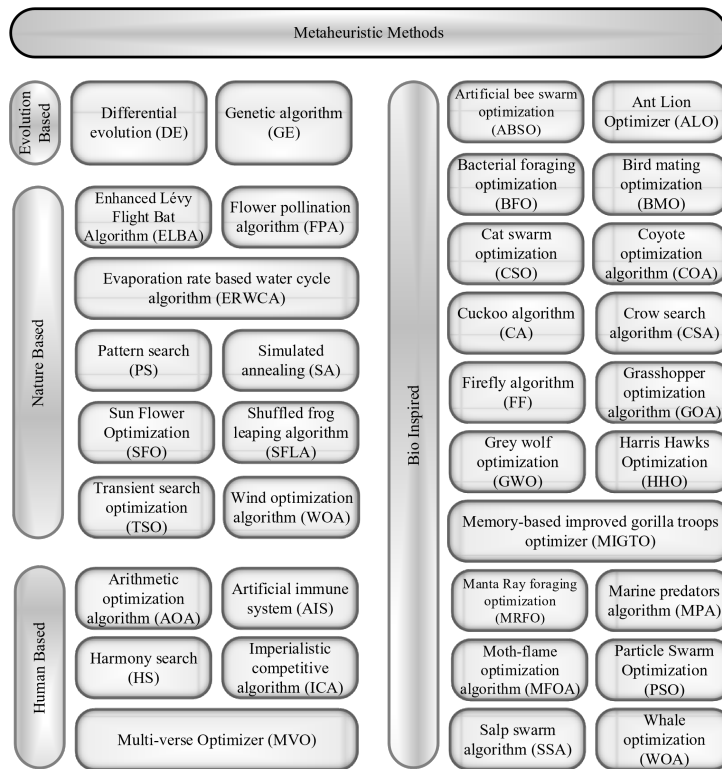


Figure 2.3: Categorizing metaheuristic algorithms used in PV parameter extraction

In the following subsections, definitions, advantages, and disadvantages of five techniques among the most commonly used ones will be given:

### a) Genetic Algorithms (GA)

Genetic algorithms (GAs) are stochastic search algorithms inspired by the basic principles of biological evolution and natural selection. GAs simulate the evolution of living organisms, where the fittest individuals dominate over the weaker ones, by mimicking the biological mechanisms of evolution, such as selection, crossover, and mutation shown in Figure (2.4). GAs have been successfully applied to solve optimization problems, both for continuous (whether differentiable or not) and discrete functions [24].

#### Advantages:

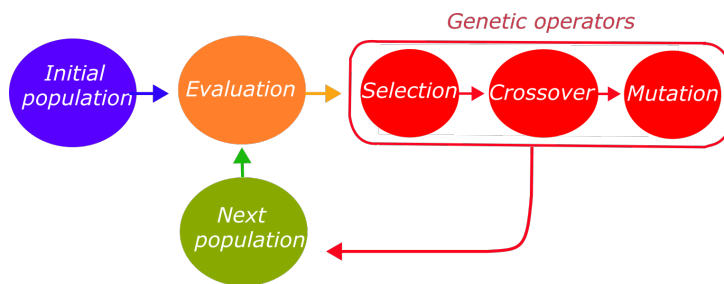


Figure 2.4: The mechanism of the Genetic Algorithms (GA)

- Fast convergence.
- It can handle a large number of variables.
- Implicit parallelism.

**Disadvantages:**

- Complicated in tuning.
- Large computational burden.

**b) Whale Optimization Algorithm (WOA)**

The Whale Optimization Algorithm (WOA) is a meta-heuristic optimization technique that is inspired by the unique hunting behavior of humpback whales known as the bubble-net feeding method. This method involves a group of humpback whales working collaboratively to encircle prey with bubbles, making it easier to capture. The WOA has been successfully applied to solve various engineering optimization problems and is known for its global optimization capabilities due to its ability to balance exploration and exploitation [25].



Figure 2.5: The mechanism of the Whale Optimization Algorithm (WOA)

**Advantages:**

- Few parameters to be tuned.
- Ability to search the entire problem space.

- Its exploration abilities can be enhanced by hybridization with other algorithms.

**Disadvantages:**

- Slow in convergence.
- Prone to premature convergence with high dimensional problems.

**c) Fuzzy logic (FL)**

Fuzzy logic provides an inference structure that accommodates human reasoning capabilities effectively. In contrast, traditional binary set theory deals with crisp events, categorizing them as either happening or not happening. Probability theory is employed in binary set theory to predict the likelihood of an event occurring. Given its simplicity and high performance in behavior modeling, FL can be applied to investigate the behavior of I-V curves in organic solar cells and extract their electrical parameters [26].

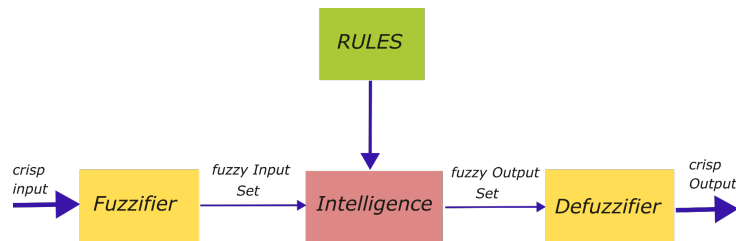


Figure 2.6: Fuzzy logic architecture

**Advantages:**

- Superior in handling uncertainties.
- Uses simple mathematics to model nonlinear and complex systems.
- Has high precision.
- Rapid in operation.

**Disadvantages:**

- Care is needed to calculate and estimate the membership function.
- To achieve more accurate results, more grades of fuzzy rules are needed. This increases the rule in an exponential manner.
- No real-time response.
- Cannot receive feedback from a learning strategy.

**d) Differential Evolution (DE)**

The Differential Evolution is a search technique based on mechanisms of natural selection and genetics [27]. Differential evolution (DE) was first introduced in the work by Storn and Price in 1997. The optimization procedure is similar to GA, but unlike GA, which relies on crossover, DE primarily utilizes the mutation operation (i.e., difference vector) as a search and selection mechanism to direct the search toward the prospective regions in the search space. Like other EA families, DE relies on initial random population generation, which is then improved using selection, mutation, and crossover [28].

**Advantages:**

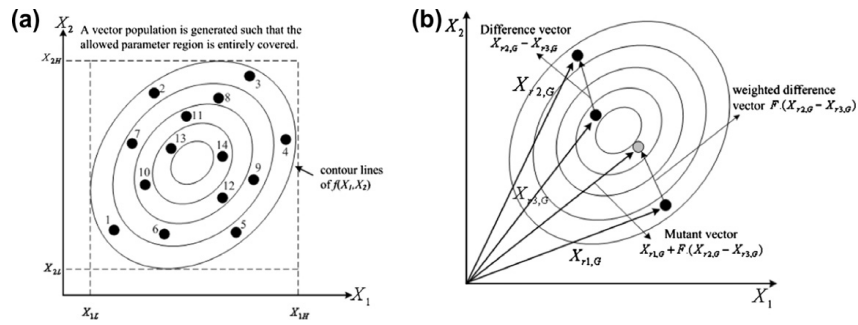


Figure 2.7: (a) Initialization of DE. (b) Mutation process of DE

- Easy to be coded.
- Fast convergence.
- For PV models, DE and its variants provide better accuracy, reliability, and computational time results.

**Disadvantages:**

- Prone to premature convergence.
- Three parameters need to be tuned.

**e) Particle Swarm Optimization (PSO)**

Particle swarm optimization (PSO) represents a stochastic swarm intelligence approach that operates on a population level, aiming to discover global optimal points through the collaborative behavior of simple agents. Unlike methods relying on system equation differentials, PSO directly explores the solution space [29].

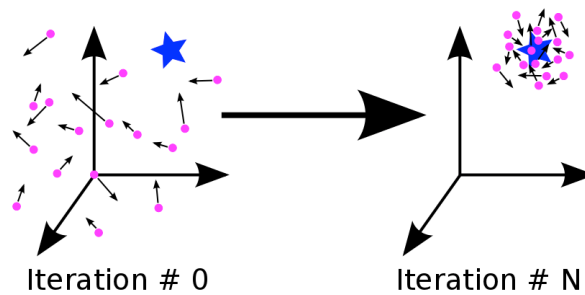


Figure 2.8: The mechanism of the Particle Swarm Optimization (PSO)

**Advantages:**

- Requires few parameters to tune.
- There is no evolution or mutation for the population.
- Requires less computation time (concerning GA).
- Its flexibility enables the balance between local and global search.

**Disadvantages:**

- Low-quality solution.
- It needs memory to update the velocities.
- Prone to premature convergence.

## 2.3 Justification for Selecting Particle Swarm Optimization (PSO) for Photovoltaic Model Optimization

Particle Swarm Optimization (PSO) has been chosen for our photovoltaic model parameter extraction due to its distinct advantages, which outweigh its drawbacks. PSO offers several significant benefits: it requires fewer parameters to tune, eliminates the need for complex operations like crossover and mutation, and provides flexibility in balancing local and global search, leading to efficient and effective optimization. These advantages make PSO particularly suitable for real-time and large-scale applications. Although PSO has some limitations, such as being prone to premature convergence and requiring memory for velocity updates, these issues can be managed through careful implementation and parameter tuning. Consequently, PSO's overall performance in terms of simplicity, computational efficiency, and robustness justifies its selection over other algorithms like Genetic Algorithms (GA), Whale Optimization Algorithm (WOA), Fuzzy Logic (FL), and Differential Evolution (DE) [5],[15].

## 2.4 Elements of Particle Swarm Optimization

In PSO, each element's movement relies on its initial value and the calculated velocity, enabling it to adjust its position throughout iterations. It evolves based on three key factors: its best neighbor, its best position, and its previous position. This evolution aims to lead the particle towards an optimal state.

Each particle is influenced by its neighborhood, which consists of a set of particles that directly affect it, particularly the one with the best criteria. At any given time, each particle knows:

- \* Its best-visited position, which primarily consists of the calculated criterion value and its coordinates.
- \* The position of the best neighbor in the swarm, representing the optimal ordering.
- \* The value it assigns to the objective function, as comparison is necessary at each iteration between the current particle's criterion value and the optimal value.

According to Maurice Clerc and Patrick Siarry, it becomes evident that a particle's evolution is essentially a combination of three types of behaviors: selfish (following its path according to its current velocity), conservative (retreating while considering its best performance), and mimetic (blindly following the best performer while considering its performance) [13].

## 2.5 Mathematical PSO equations

Within PSO, a group of particles navigates an unknown space, their velocities adjusted through a combination of inertia, self-awareness, and social interaction. At each iteration, the velocity and position of each particle evolve according to the following equations [30]:

$$v_i(k) = \omega \cdot v_i(k) + c_1 \cdot \text{rand}() \cdot (p_{\text{best},i} - x_i(k)) + c_2 \cdot \text{rand}() \cdot (g_{\text{best}} - x_i(k)) \quad (2.1)$$

$$x_i(k+1) = v_i(k) + x_i(k) \quad (2.2)$$

Where,  $x_i$  represents the position of the  $i$ -th particle in the variable space,  $v_i$  denotes the velocity of the  $i$ -th particle,  $\omega$  stands for the particle inertia,  $c_1$  denotes the cognitive acceleration constant,  $c_2$  represents the social acceleration constant,  $p_{\text{best}}$  signifies the particle's best-known position,  $g_{\text{best}}$  denotes the best-known position discovered by all particles, and  $\text{rand}()$  generates a random number between 0 and 1.

The impact of the three parts of equation 2.1 as described as follows:

$\omega \cdot v_i(k)$ : inertia term. It maintains the particle's current direction of movement to some extent.

$c_1 \cdot \text{rand}() \cdot (p_{\text{best},i} - x_i(k))$ : cognitive component. It drives the particle towards its own best-known position.

$c_2 \cdot \text{rand}() \cdot (g_{\text{best}} - x_i(k))$ : social component. It pulls the particle towards the best-known position found by any particle in the swarm.

The process of velocity formation and position update is depicted in Figure 2.9.

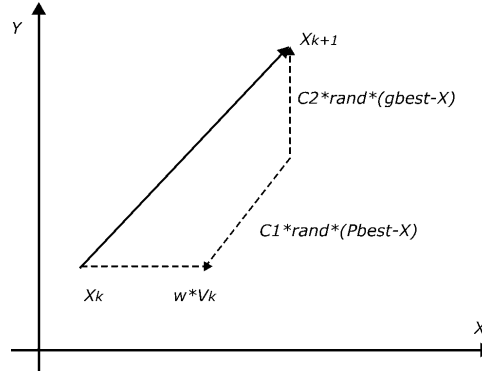


Figure 2.9: Velocity formation and position update in PSO

## 2.6 Explanation of Particle Swarm Optimization (PSO) Elements

The following subsection gives a more thorough explanation of the inertia factor ( $w$ ) and the confidence coefficients ( $c_1, c_2, r_1, r_2$ ).

### A. Inertia Factor

Particle initialization is essential for reaching the optimal solutions. For each inertia factor value, a new search space is explored. Using different paths yields the best results; therefore, the inertia factor, with a range of  $0 < w < 1$ , is crucial in the velocity equation [31].

### B. Confidence Coefficients

The acceleration coefficients  $c_1$  and  $c_2$  multiplied by the random values  $r_1$  and  $r_2$  give controllable stochastic influences on the speed of the swarm, i.e., they control the direction of a particle so that it moves to its best position  $P_{\text{best},i}(t)$  or the best position of the whole set  $G$ , with  $0 < \frac{c_1 + c_2}{2} < 1$  [31].

### C. Parameters Adjustment

To obtain good results, PSO requires setting some parameters before the start of the algorithm to improve performance. The parameters involved are:

- The number of particles in the swarm.
- The maximum speed of a particle.
- The empirical parameters  $w$ ,  $c_1$ ,  $c_2$ ,  $r_1$ ,  $r_2$ .
- The stopping criteria (the number of iterations, the improvement rate, a satisfactory solution is found). In our case, decisions are made with several tests to find the ideal values [31].

## 2.7 Conclusion

In this chapter, we focused on the identification of parameters for photovoltaic panels. We presented two main types: analytical methods and metaheuristic methods. Opting for metaheuristic methods, we introduced some of their algorithms, namely Genetic Algorithms (GA), Simulated Annealing (SA), Fuzzy logic (FL), Differential Evolution (DE), and Particle Swarm Optimization (PSO). We outlined the advantages and disadvantages of each algorithm, ultimately selecting Particle Swarm Optimization. We provided an overview of Particle Swarm Optimization, explaining its elements.

## Introduction

As discussed in Chapter Two, accurately modeling a PV module requires the extraction of several parameters. This modeling is crucial not only for educational purposes but also for evaluating the performance of a PV panel. The process of parameter extraction for PV models is inherently complex, involving multiple variables and nonlinear, multi-modal problems. This challenge has garnered significant attention in the simulation and analysis of solar PV systems.

Parameters can be extracted using either metaheuristic or analytical algorithms based on the actual experimental data. In this project, the metaheuristic Particle Swarm Optimization (PSO) algorithm has been adopted due to its advantages mentioned in the second chapter, to extract the parameters of a single diode model using experimental data. This chapter will detail the various steps of parameter extraction, starting with obtaining experimental data, developing the mathematical equations necessary for the PSO calculations, and finally, generating the I-V and P-V characteristics.

### 3.1 Panel Parameters Extraction Based on PSO Algorithm

This section outlines the various steps the PSO algorithm follows to calculate three parameters: shunt resistance ( $R_{sh}$ ), series resistance ( $R_s$ ), and the ideality factor ( $n$ ). Initially, different equations are developed, starting with the current equation and leading up to the predicted current equation, which contains five unknown parameters ( $R_{sh}$ ,  $R_s$ ,  $n$ , and the measured panel values  $V_d$  and  $I_d$ ).

A PV cell is modeled by a current source in parallel with a diode, accompanied by a shunt resistor and a series resistor to account for internal loss mechanisms [16]. The current generated by a PV cell can be described as the current from the source minus the current through the diode and the shunt resistor:

$$I = I_{ph} - I_D - I_{sh} \quad (3.1)$$

The diode current  $I_D$  is given by:

$$I_D = I_0 \left( e^{\frac{q(V + R_s I)}{n k T}} - 1 \right) \quad (3.2)$$

The shunt resistor current  $I_{sh}$  is:

$$I_{sh} = \frac{V + R_s I}{R_{sh}} \quad (3.3)$$

The PSO algorithm necessitates the specification of a metric to assess the performance of each particle. In this context, the objective is to align model parameters with a set of sampled points. Hence, the discrepancy between the model's predictions and the corresponding actual measurements will be evaluated through a fitness function. Field test data typically includes three points on the V-I curve of a PV cell: the open-circuit point, the short-circuit point, and a load point. At open circuit ( $I = 0$ ), assuming a high enough shunt resistance to neglect the final term in the first equation, the open-circuit voltage  $V_{oc}$  is [30]:

$$V_{oc} = \frac{nkT}{q} \ln \left( \frac{I_{ph}}{I_0} + 1 \right) \quad (3.4)$$

At short circuit ( $V = 0$ ), assuming a low enough series resistance and high enough shunt resistance, the short-circuit current  $I_{sc}$  is:

$$I_{sc} = I_{ph} \quad (3.5)$$

According to the previous equations and by using the open-circuit voltage ( $V_{oc}$ ) and short-circuit current ( $I_{sc}$ ) sampled from the PV cell, we can derive an expression for the reverse saturation current ( $I_0$ )[30]:

$$I_0^* = \frac{I_{sc}}{e^{\frac{qV_{oc}}{nkT}} - 1} \quad (3.6)$$

Next, substituting  $I_0^*$  into the original equations gives the expected load current:

$$I^* = I_{sc} - I_0^* \left( e^{\frac{q(V_d + I_d R_s^*)}{n^* k T_d}} - 1 \right) - \frac{V_d + I_d R_s^*}{R_{sh}^*} \quad (3.7)$$

Where:

- $I_0^*$  is the predicted reverse saturation current,
- $I^*$  is the predicted load current,
- $I_d$  is the sampled load current,
- $V_d$  is the sampled load voltage,
- $I_{sc}$  is the sampled short-circuit current,
- $V_{oc}$  is the sampled open-circuit voltage,
- $T_d$  is the sampled environmental temperature,
- $n^*$ ,  $R_s^*$ , and  $R_{sh}^*$  are the PV parameters to be determined.

### 3.1.1 Fitness function

To evaluate the discrepancy between the model's predictions and the actual measurements, the fitness function is used. This involves minimizing the quadratic error between the measured current and the current calculated from the adopted PV model. The fitness function is based on the fitness metric of

each particle. This equation will compare the predicted load current ( $I^*$ ) to the actual sampled load current ( $I_d$ ). So, the fitness function for one sampled point is defined as:

$$f_i = |I^* - I_d| \quad (3.8)$$

For a set of  $N$  sampled points, the overall fitness function is:

$$f = \sqrt{\sum_{i=0}^N f_i^2} \quad (3.9)$$

In this way, the PSO algorithm searches for the optimal set of PV parameters ( $R_{sh}$ ,  $R_s$ ,  $n$ ), that minimize the error with respect to the sampled data [30].

### 3.1.2 Definition of parameters search space

In this study, the proposed optimizing algorithm searches for an optimal set of PV parameters to minimize errors respect to the sampled data. Each particle contains a vector of parameters to be optimized:  $R_{sh}$ ,  $R_s$ ,  $n$ . The search space for each of the three parameters, which is defined based on common sense and gained experience, is given is Table (3.1).

Table 3.1: Search space area definitions

<b>n</b>	$R_s$ [ $\Omega$ ]	$R_{sh}$ [ $\Omega$ ]
0 - 2	0 - 20	10 - 200

### 3.1.3 PSO parametrs definition

In PSO, the concept of weight inertia is crucial for managing both the initial exploration and eventual exploitation phases of optimization. The formula of weight inertia, denoted as  $\omega$ , used in this application is given by the flowon equation :

$$\omega = 0.8 - 0.4 \times \frac{\text{iteration}}{\text{max\_iteration}} \quad (3.10)$$

where "iteration" represents the current iteration number, and "max\_iteration" is the total number of iterations.

Individual and social acceleration constants are set to 2.0. Maximum velocity is set to half of the search space for each dimension. The number of particles is set to 50, and the maximum number of iterations is 100 [30].

### 3.1.4 PSO processing steps

The various steps for implementing PSO are illustrated in the flowchart shown in Figure (3.1), starting from the initialization of 50 particles to the attainment of the three parameters  $R_{sh}$ ,  $R_s$ ,  $n$ .

## 3.2 Simulation results

In the first step for validating our PSO program, the sampled point data were extracted from the model panel in the Simulink/MATLAB environment, specifically the 'Panasonic Eco Solution PE240M-BBB

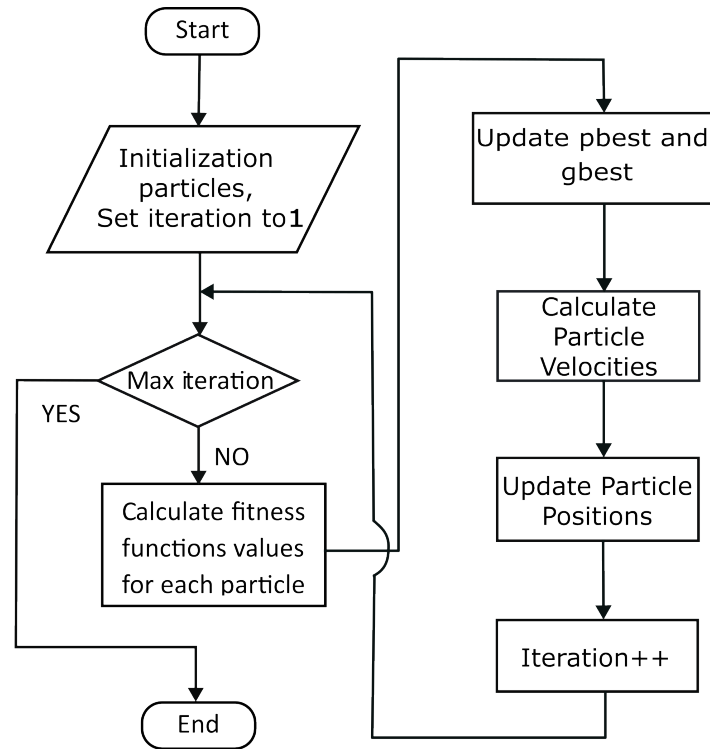


Figure 3.1: Flowchart of the PSO program

panel'. The technical characteristics of this panel under standard test conditions (STC: temperature of 25°C and irradiance of 1000 W/m<sup>2</sup>) are listed in Table (3.2).

The 100 points extracted from the previously mentioned panel model represent the voltage ( $V_d$ ) and the current ( $I_d$ ), which are utilized in Equation (3.7). These voltage and current data points are indispensable for computing the predicted current and determining the fitness value.

The I-V and P-V curves of the used panel model under the STC conditions are presented in Figures (3.2),(3.3) respectively.

Parameter	Value
Power (P)	240 W
Short-circuit current (Isc)	8.71 A
Open-circuit voltage (Voc)	36.97 V
Maximum current (Imax)	7.97 A
Maximum voltage (Vmax)	30.2 V
Temperature coefficient of Isc	0.036005
Temperature coefficient of Voc	-0.34501
Number of solar cells	60
Cell type	Monocrystalline

Table 3.2: Specification of the Panasonic Eco Solution PE240M-BBB at STC condition

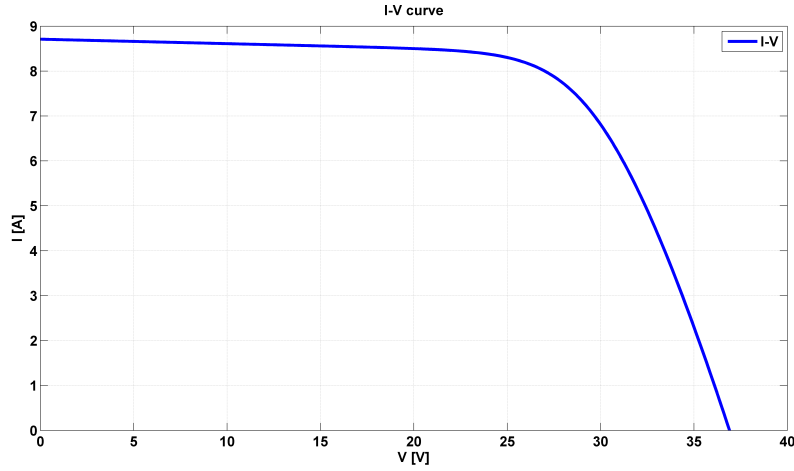


Figure 3.2: The I-V characteristic curve of Panasonic PE240M-BBB panel under STC conditions

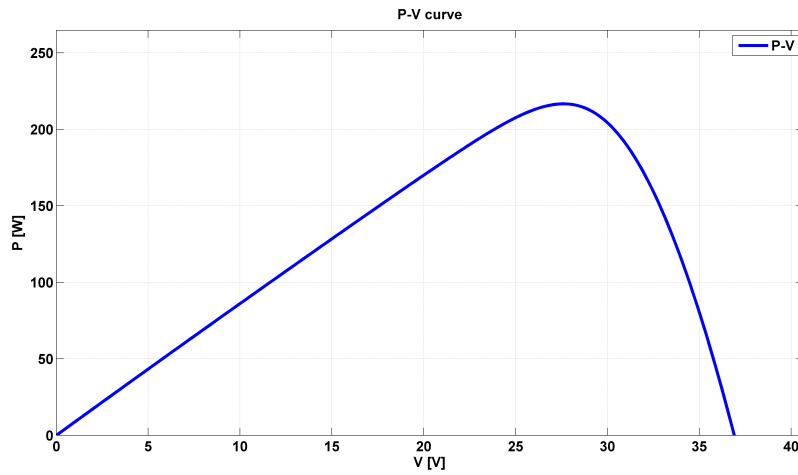


Figure 3.3: The P-V characteristic curve of Panasonic PE240M-BBB panel under STC conditions

### 3.3 Predicted I-V Characteristic Curve

After running the PSO program using the sampling points from the chosen panel model, the three obtained parameters ( $R_s$ ,  $R_{sh}$ ,  $n$ ) are listed in Table (3.3). These parameters have been used to formulate the mathematical equation of the panel. MATLAB code was then written to plot the curve of the resulting equation. Figure (3.4) depicts the I-V characteristics of both the predicted and MATLAB model panels.

Table 3.3: Obtained PV panel Parameters using PSO Algorithm

$n$	$R_s$ [ $\Omega$ ]	$R_{sh}$ [ $\Omega$ ]
1.10	0.22	98.32

From Figure 3.4, it is clear that the predictive I-V curve and the MATLAB model curve overlap, confirming the accuracy of the obtained parameters and the efficiency of the PSO technique. Thus, the predictive model serves as a valuable tool for simulating the real operation of panels, allowing for a better understanding and optimization of photovoltaic system performance.

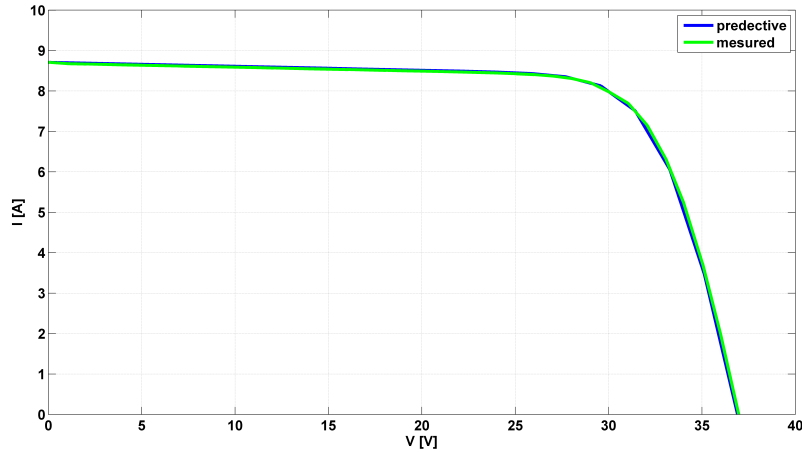


Figure 3.4: Predicted I-V characteristic curve of the Panasonic Eco Solution PE240M-BBB panel

### 3.4 Impact of Temperature and Irradiance on PV Model Prediction

Considering that PV panels constantly operate under varying irradiance and temperature, it becomes impractical to measure the sampled data points used in the prediction process under the STC conditions. Therefore, it is necessary to measure this data under real conditions. The impact of the atmospheric conditions will be incorporated into the equations of the affected parameters.

To reaffirm the impact of varying temperature and irradiance on the I-V characteristic, both the I-V characteristics under STC and under conditions of  $800 \text{ W/m}^2$  and  $35^\circ\text{C}$  are plotted together in Figure (3.5).

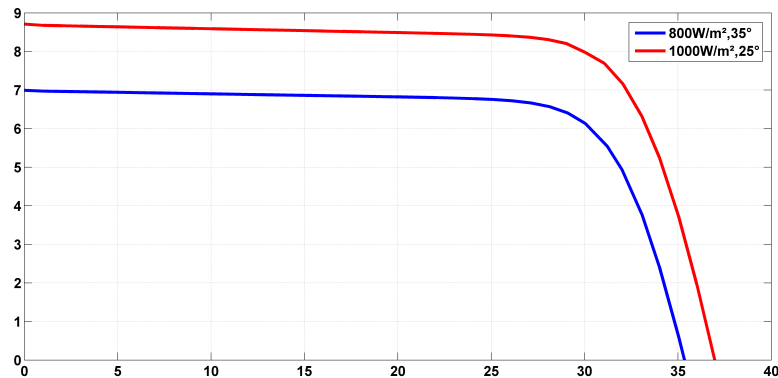


Figure 3.5: Impact of temperature and irradiance on the photovoltaic current

After using equations (1.28), (1.29), and (1.31) to develop the equation for the predictive current and running the PSO program with the sampled points from the panel model at  $800 \text{ W/m}^2$  and  $35^\circ\text{C}$ , the three obtained parameters ( $R_s$ ,  $R_{sh}$ , and  $n$ ) are listed in Table (3.4).

Both the predictive I-V curve and the MATLAB model I-V curve of the Panasonic PE240M-BBB panel under  $800 \text{ W/m}^2$  and  $35^\circ\text{C}$  are depicted in Figure (3.6).

The results of the predictive model under  $800 \text{ W/m}^2$  and  $35^\circ\text{C}$  reaffirm the capability of the PSO algorithm in accurately determining the PV panel parameters.

Table 3.4: Obtained PV panel Parameters for Panasonic PE240M-BBB Panel under  $800 \text{ W/m}^2$  and  $35^\circ\text{C}$

$n$	$R_s [\Omega]$	$R_{sh} [\Omega]$
1.20	0.14	94.96

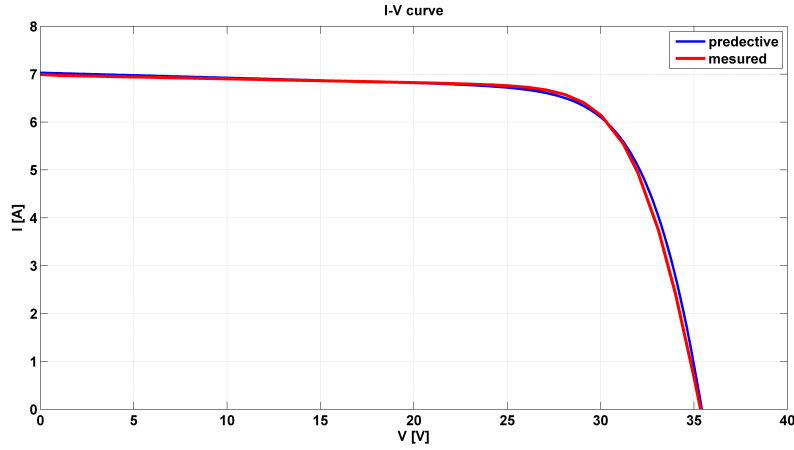


Figure 3.6: Predictive I-V Curve Showing the Impact of Temperature and Irradiance Using PSO-Extracted Parameters

## 3.5 Real panel parameters identification

To confirm the efficiency of the PSO algorithm in extracting real PV panel parameters, as demonstrated with MATLAB models under both STC conditions and varying atmospheric conditions, this part of our project is dedicated to the experimental validation of the used technique. The first step is to obtain real panel sample points data. This data allows us to draw the I-V characteristic curve of the real panel and calculate the fitness value.

### 3.5.1 Sampling points data measurement

To draw the I-V characteristic curve of a real panel, different techniques can be used. This can be done directly using an I-V characteristic tracer instrument, or by connecting a rheostat or a capacitor to the PV panel and measuring the current while varying the resistance value. Starting from its lower values (approximately  $0\Omega$ ), which gives the short circuit current ( $I_{sc}$ ), to its maximum values (approaching infinity), which allows for obtaining the open circuit voltage ( $V_{oc}$ )[32].

In our case, due to the lack of an I-V characteristic tracer instrument in our laboratory, we adopted the basic principle of varying a rheostat from a very large value to a very small value to measure the corresponding current and voltage values, including the short-circuit current and open-circuit voltage.

### 3.5.2 I-V characteristic measurement setup

The setup used in our study is part of the solar energy kit of the Mechanics Laboratory at the University of Mohamed Boudiaf-Msila. It is composed of the instruments shown in Figure 3.7 and listed below:

- Adjustable and mobile chassis

- Digital display measuring devices
- Variable resistor
- Solar module
- Temperature sensor
- Light sensor
- Solar module connections

The photovoltaic module used in the setup is of the monocrystalline type, with its parameters listed in Table (3.5). The panel is equipped with temperature and irradiance sensors. Their values, along with the PV module current and voltage, can be directly read by the apparatus shown above the rheostat in Figure (3.7). For the load, three rheostats of  $33\Omega$  were connected in series to achieve a varying resistance of  $100\Omega$ .

### 3.5.3 sampling points data measurement procedure

To obtain all the required points to draw the I-V characteristic curve of the panel, the first point to be measured is the short circuit current  $I_{sc}$ , and the last point should be the open circuit voltage  $V_{oc}$ . Initially, the equivalent rheostat was set to a low value of  $0.5\Omega$ , which resulted in a current of  $4.44\text{A}$  and a voltage of  $2.9\text{V}$ . The resistance was then gradually increased, measuring the corresponding current and voltage values until reaching the maximum resistance value of  $100\Omega$ , which gave a current of  $0.19\text{A}$  and a voltage of  $19.43\text{V}$ .

A total of 86 points were measured, all under nearly constant temperature and irradiance values of  $32^\circ\text{C}$  and  $560\text{W}/\text{m}^2$ , respectively.

Table 3.5: Specifications of Module 85W at STC condition

Parameter	Value
Power (P)	85 W
Short-circuit current (Isc)	5.11 A
Open-circuit voltage (Voc)	21.96 V
Maximum current (Imax)	4.65 A
Maximum voltage (Vmax)	18.29 V
Number of solar cells	36
Cell type	Monocrystalline

The obtained I-V curve of the setup panel (ET-M53685) under  $32^\circ\text{C}$  and  $560\text{W}/\text{m}^2$  is shown in Figure (3.8):

The measured sample points, along with atmospheric parameters, are input into the PSO code designed for non-STC conditions. After running the code, the three obtained parameters ( $R_s$ ,  $R_{sh}$ , and  $n$ ) are listed in Table (3.6).

The three obtained parameter values were fed into the MATLAB code to generate a plot showing both curves: the predictive current curve and the curve representing the real panel. Figure (3.9) presents these two curves, demonstrating their overlap, with only minor differences observed in the slope of the curve shape. These discrepancies may be deemed negligible errors, or one may opt to adjust the  $R_s$  value to remove this error.



Figure 3.7: Laboratory Setup

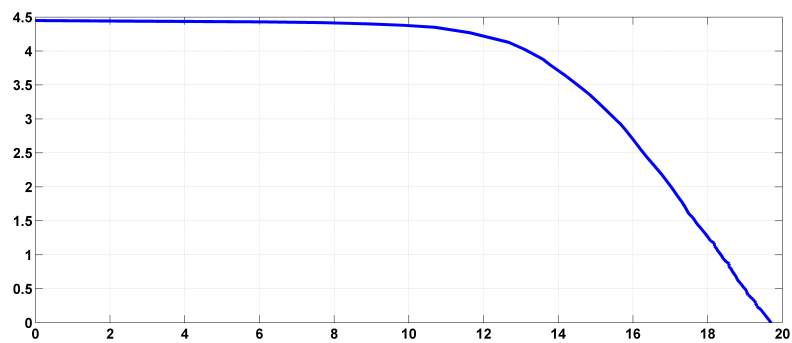


Figure 3.8: Real PV panel (ET-M53685) I-V curve

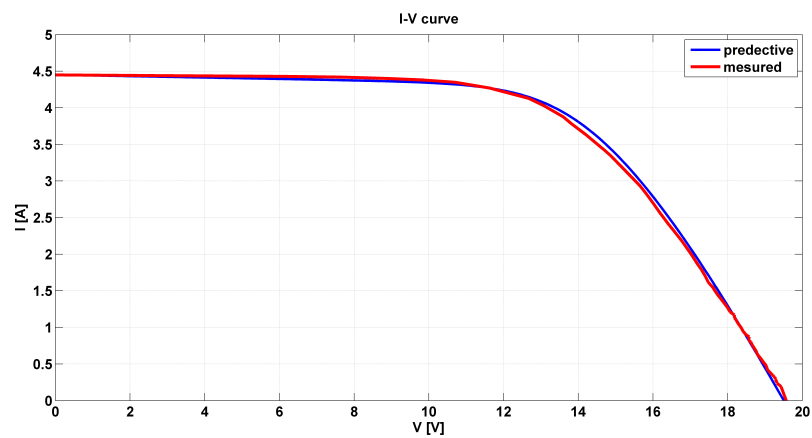


Figure 3.9: Real and predicted I-V characteristic curve of ET-M53685 panel

Table 3.6: Obtained PV panel Parameters for setup panel ET-M53685

<b>n</b>	$R_s[\Omega]$	$R_{sh}[\Omega]$
1.07	0.88	105.4

### 3.6 Conclusion

In this chapter, the implementation and validation of the PSO algorithm for extracting parameters of a PV module were comprehensively discussed. The chapter began with a detailed explanation of the implementation of the PSO algorithm for PV panel parameter extraction and the different processing steps. Subsequently, simulation results obtained from the Panasonic Eco Solution PE240M-BBB model panel were presented, highlighting the effectiveness of the PSO algorithm in accurately predicting the I-V characteristic curve. Furthermore, the prediction of the three panel parameters under varying temperature and irradiance conditions was analyzed, demonstrating the algorithm's effectiveness in varying environmental conditions. The experimental setup and procedure for measuring the I-V curve of the real panel were also described, and the use of these real panel data to extract its parameters with the PSO algorithm was extensively discussed. Finally, a comparison between the predicted and experimental I-V curves was made, confirming the accuracy of the PSO algorithm in PV panel parameter extraction for both the MATLAB PV panel model and the real ones.

## GENERAL CONCLUSION

The research conducted in this thesis revolves around the identification of photovoltaic module parameters for simulation application, focusing on the construction and modeling of photovoltaic panels.

The initial chapters laid the foundation by delving into the historical background of photovoltaic energy and elucidating the photovoltaic effect. Semiconductor fundamentals, including the formation of the PN junction, were explored, leading to an understanding of the principal photovoltaic conversion process. Furthermore, various photovoltaic cell technologies and their electrical characteristics were examined, along with the association of photovoltaic cells. The chapter concluded with insights into the modeling of photovoltaic cells and the influence of climatic parameters on module performance.

Moving forward, techniques for parameter extraction of photovoltaic panels were investigated in Chapter 2. This included an in-depth discussion on solar cells I-V explicit equations, analytical methods, and metaheuristic methods for parameter identification. The principles of Particle Swarm Optimization (PSO) were elucidated, along with the mathematical equations governing PSO. Moreover, the chapter elaborated on the implementation of PSO, including the definition of fitness functions and particle and search space definition.

Chapter 3 focused on simulating and experimenting with the proposed methodologies. The principle of the PSO algorithm was outlined, along with simulation results and the predicted I-V characteristic curve using the PSO algorithm. Additionally, the impact of temperature on photovoltaic performance was analyzed, and the experimental technique for measuring the current-voltage (I-V) curve was discussed.

In conclusion, this thesis has contributed to advancing the understanding of photovoltaic module parameters for simulation application. Through theoretical exploration and practical experimentation, the effectiveness of the proposed methodologies has been demonstrated. As the world continues to shift towards renewable energy sources, the insights gained from this research are instrumental in the development of efficient photovoltaic systems.

From a research perspective, several avenues for further investigation are recommended:

- Deepening investigations into the long-term impact of environmental factors on photovoltaic module performance.
- Exploring more advanced metaheuristic methods for parameter identification.
- Developing real-time monitoring systems for photovoltaic panels to improve efficiency and maintenance.
- Expanding the study to include diverse photovoltaic technologies and their applications in various

climatic conditions.

These perspectives not only build on the current findings but also pave the way for future innovations and improvements in photovoltaic technology.

The increasing global demand for renewable energy solutions has intensified research into optimizing photovoltaic (PV) systems. Accurate modeling of PV modules is essential for predicting their performance and enhancing the efficiency of solar energy systems. This dissertation addresses the identification and extraction of key PV module parameters using Particle Swarm Optimization (PSO) within the single diode model. The study focuses on extracting five critical parameters: diode ideality factor ( $n$ ), series resistance ( $R_s$ ), shunt resistance ( $R_{sh}$ ), photocurrent ( $I_{ph}$ ), and reverse saturation current ( $I_0$ ). The PSO algorithm, inspired by social behaviors of birds flocking or fish schooling, optimizes this process by minimizing errors between experimental data and the model. Validation using experimental data under various conditions highlights PSO's effectiveness in precise parameter identification, enhancing the reliability of PV simulations. The research provides practical guidelines for implementing PSO in PV parameter extraction, contributing to the advancement and broader adoption of solar energy systems.

Key words: Photovoltaic - Parameters identification- single-diode model- PSO algorithm.

## BIBLIOGRAPHY

- [1] Kenu E. Sarah, Prof. Uhumwangho Roland, and Prof. Okafor Ephraim N. C. A review of solar photovoltaic technologies. *International Journal of Engineering Research and Technology (IJERT)*, 2020.
- [2] OM PRAKASH MAHELA and SHEESH RAM OLA. Modeling and control of grid-connected photovoltaic systems. *International Journal of Engineering Research and Technology (IJERT)*, 2013.
- [3] BAKHTAOUI Djamila and ALLAL Siham. Modeling and control of a grid-connected photovoltaic system. Master's thesis, Université Mohamed Boudiaf - M'sila, 2022/2023.
- [4] Wei Zhou, Pengjun Wang, Ali Asghar Heidari, Xuehua Zhao, Hamza Turabieh, and Huiling Chen. Random learning gradient-based optimization for efficient design of photovoltaic models. *Journal of Photovoltaic Engineering*, 2021.
- [5] Samuel R. Fahim, Hany M. Hasanien, Rania A. Turky, Shady H. E. Abdel Aleem, and Martin Calasan. A comprehensive review of photovoltaic modules models and algorithms used in parameter extraction. *Renewable Energy*, 2022.
- [6] BENKHERIF Abdelbacet and SEDDIKI Benyoucef. Étude technico-Économique d'un système photovoltaïque en site isolé par pvsyst. Master's thesis, Université Mohamed Boudiaf - M'sila, 2017/2018.
- [7] MECHAI Fazia. *Etude et simulation des structures photovoltaïques à base de chalcogénures de métaux de transition MX<sub>2</sub> (M = W, Mo; X = S, Se)*. Mémoire de magister, Université Mouloud Mammeri de Tizi-Ouzou, 2016.
- [8] SLAMA Fateh. *Modélisation d'un système multi générateurs photovoltaïques interconnectés au réseau électrique*. Mémoire de magister, Université Ferhat Abbas - Setif, 2011.
- [9] DIDA Mustapha. *Etude et amélioration des systèmes de conversion photovoltaïque dans les zones arides et semi-arides*. Doctrat thesis, Université Kasdi Merbah Ouargla, 2021/2022.
- [10] Oz Yakrangı. *Design and comparative analysis of different solar cell technologies of a 3 MW Grid-Connected PV system*. Master's thesis, Escola Tècnica Superior d'Enginyeria Industrial de Barcelona, 2017 /2018.
- [11] *Technical Application Papers No.10 Photovoltaic plants*. book, 2010.

- [12] D. W. de Lima Monteiro T. M. Barcelos and M. F. V. Lessa. *Analytical Model for a Mixed Association of Photovoltaic Cells*. Article, 2008.
- [13] ARBOUCHE Riadh et AICHI Mohieddine. *Identification des paramètres d'un module photovoltaïque*. Memoire master, Universite Kasdi Merbah Ouargla, 2021/2022.
- [14] Dr. Ali N. Hamoodi, Safwan A. Hamoodi, and Rasha A. Mohammed. *Photovoltaic Modeling and Effecting of Temperature and Irradiation on I-V and P-V Characteristics*. Article in international journal of applied engineering research, 2018.
- [15] HARRAG Abdelghani and MESALTI Sabir. *Three, Five and Seven PV Model Parameters Extraction using PSO*. International conference on technologies and materials for renewable energy, 2017.
- [16] Jing Jun Soon and Kay-Soon Low. *Photovoltaic Model Identification Using Particle Swarm Optimization With Inverse Barrier Constraint*. Article in iee, 2012.
- [17] Miqdam Tariq Chaichan Moafaq Kaseim Al-Ghezi and Roshen Tariq Ahmedhamdi. *The Influence of Temperature and Irradiance on Performance of the Photovoltaic Panel in the Middle of Iraq*. Article in international journal of renewable energy development, 2022.
- [18] Mame Fadiamé THIAM Babou DIONE, Mountaga BOIRO. *Influence of Temperature on the Serial and Shunt Resistance of a Silicon Solar Cell under Polychromatic Illumination in Static Mode*. Article in ira-international journal of applied sciences, 2022.
- [19] BAADJI Ahlam et CHERGUI Imane. *Extraction des Paramètres du Module Photovoltaïque*. Memoire master, Universite Mohamed Boudiaf - M'sila, 2018/2019.
- [20] KOUTB-EDDINE BOUTRIK. *PV Parameters extraction using Metaheuristics*. Master's thesis, University M'hamed Bougara – Boumerdes, 2020.
- [21] Hany M. Hasanien Bahaa Saad Mahmoud A. El-Dabah, Ragab A. El-Sehiemy. *Photovoltaic model parameters identification using Northern Goshawk Optimization algorithm*. Article, 2022.
- [22] Jose M. Blanes F. J. Toledo. *Analytical and quasi-explicit four arbitrary point method for extraction of solar cell single-diode model parameters*. Article, 2016.
- [23] Mohamed Ali Abdelkareem Hussein M Maghrabie Ahmed M. Nassef, Ahmad Baroutaji. *Review of methauristic optimization algorithms for power systems problems*. Review, 2023.
- [24] Luca Scrucca. *A Package for Genetic Algorithms in R*. Journal article, 2013.
- [25] Mohamed A. Elgendy Amr M. Abdeen Omnia S. Elazab, Hany M. Hasanien. *Whale optimisation algorithm for photovoltaic model identification*. The 6th international conference on renewable power generation (rpg), 2017.
- [26] D. Arar T. Bendib, F. Djefal and M. Meguellati. *Fuzzy-Logic-based Approach for Organic Solar Cell Parameters Extraction*. Article, 2013.
- [27] Fardie J. F. et all de Costa, W. T. *Identification of photovoltaic model parameters by differential evolution*. Article in iee international conference, 2010.

- [28] Kashif Ishaque and Zainal Salam. *An improved modeling method to determine the model parameters of photovoltaic (PV) modules using differential evolution (DE)*. Article in elsevier, 2011.
- [29] Hengsi Qin and Jonathan W. Kimball. *Parameter Determination of Photovoltaic Cells from Field Testing Data using Particle Swarm Optimization*. Article in iee, 2011.
- [30] Ahmed Abderrahmane BOUDJENANA Lyes ABADA, Merouane BENNACEUR and Saliha AOuat. *Using PSO metaheuristic to solve photometric 3D reconstruction*. Article in iee, 2022.
- [31] Fernando M. Janeiro Abdeloawahed Hajjaji and Khalid Kandoussi Oumaima Mesbahi, Mouhaydine Tlemçani. *A Modified Nelder-Mead Algorithm for Photovoltaic Parameters Identification*. International journal of smart grid, 2020.
- [32] Areej Ahmad Alia. *Predicting I-V curve for photovoltaic modules using Random Forests Technique*. Master's thesis, An Najah National University, Nablus Palestine, 2020.